CrystEngComm

PAPER

View Article Online
View Journal | View Issue

Cite this: *CrystEngComm*, 2015, **17**, 1080

Carbon nanodots functional MOFs composites by a stepwise synthetic approach: enhanced H_2 storage and fluorescent sensing†

Ji-Sen Li,[ab] Yu-Jia Tang,[a] Shun-Li Li,[a] Shu-Ran Zhang,[c] Zhi-Hui Dai,*[a] Ling Si[a] and Ya-Qian Lan*[a]

Received 8th October 2014,
Accepted 19th November 2014

DOI: 10.1039/c4ce02020k

www.rsc.org/crystengcomm

Metal–organic frameworks (MOFs) hybrid composites, combining the advantages of both MOFs and nanoparticles, may exhibit unprecedented properties. Herein, carbon nanodots (Cdots) functional UMCM-1 composites (Cdots@UMCM-1a) were successfully synthesized by a stepwise synthetic approach for the first time. The hybrids retain the intact structure of MOFs with high luminescence and longer stability. Due to the interactions between polar functional groups at the surface of the Cdots and H_2 molecules, Cdots@UMCM-1a efficiently enhanced H_2 storage capacity. Most importantly, Cdots@UMCM-1a exhibited highly fluorescent sensing for nitroaromatic explosives owing to the double effect of porous MOFs and fluorescent Cdots. This work will pave new avenues for the fabrication of novel and multifunctional MOFs composites.

Introduction

Metal–organic frameworks (MOFs), which are characteristic of an emerging family of porous materials, have attracted much attention during the past few decades.[1] Owing to some unique advantages of MOFs, such as high surface areas,[2] tunable pore sizes,[3] and versatile structures,[4] MOFs can reasonably be widely applied in gas storage or separations,[5] catalysis,[6] and others.[7] Nonetheless, MOFs have some shortcomings such as poor thermal and chemical stability, which limit their potential applications to a very large extent. In recent years, many efforts have been dedicated to overcoming these drawbacks as well as introducing novel functionalities. Fortunately, MOFs hybrid composites, combining the advantages of both excellent adsorption capacities from MOFs and different functionality from nanoparticles and imparting unprecedented properties, have been obtained to date.[8] These nanoparticles consist of metal nanoparticles,[9] graphene,[10] carbon nanotubes,[11] polyoxometalates,[12] and quantum dots.[13] Thus, fabricating novel nanoparticles functional MOFs composites with intriguing properties will provide new impetus for synthesizing and applying these composites in future.

Recently, carbon nanodots (Cdots) as a rising star have drawn particular interest due to their fascinating fluorescent properties and low toxicity.[14] Especially, the synergistic combination of the merits of both MOFs and Cdots, Cdots functional MOFs composites (Cdots@MOFs) possess many novel properties superior to those of the individual components as follows: 1) based on the ultrahigh porosities and surface areas of MOFs and high fluorescence of Cdots, Cdots@MOFs are expected to be applied in biosensing, fluorescent sensors, and other applications; 2) the polar functional groups on Cdots surface may also combine with metal ions, and further modulate the growth of MOFs as crystallization seeds.[13d] Therefore, the introduction of Cdots into MOFs, and adding a new active point for MOFs materials, will become a new direction in the Cdots and MOFs sciences in the future.

At present, many applications of synthesized MOFs are limited because the crystals are relatively large in size (μm–mm). However, the smaller-sized MOFs and/or nanoparticles functional MOFs may provide promising applications such as optical sensors,[13a] size-selective SERS,[15] and others.[16] Despite tremendous efforts, to the best of our knowledge, the construction of smaller-sized Cdots@MOFs composites remains largely unexplored to date. Based on the above considerations, it is a scientific and technological challenge to synthesize smaller-sized and highly fluorescent Cdots@MOFs as a fluorescent sensing material.

Herein, for the first time, we obtained highly fluorescent Cdots@UMCM-1 composites by a stepwise synthetic method

[a] *Jiangsu Key Laboratory of Biofunctional Materials, College of Chemistry and Materials Science, Nanjing Normal University, Nanjing 210023, PR China. E-mail: yqlan@njnu.edu.cn, daizhihuii@njnu.edu.cn*
[b] *Department of Chemistry and Chemical Engineering, Jining University, Qufu 273155, PR China*
[c] *Institute of Functional Material Chemistry, Faculty of Chemistry, Northeast Normal University, Changchun 130024, PR China*

† Electronic supplementary information (ESI) available: Figures and tables. See DOI: 10.1039/c4ce02020k

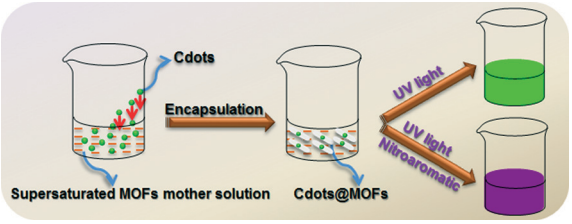

Scheme 1 Schematic illustration of Cdots@MOFs composites.

(Cdots@UMCM-1a, Scheme 1). In particular, the sizes of the Cdots@UMCM-1a are approximately one twentieth of those of the hybrids by a solvothermal approach. Due to the cumulative effect of UMCM-1 and Cdots, it appears to be unprecedented that Cdots@UMCM-1a show the fast and enhanced fluorescent sensing for nitroaromatic explosives. Moreover, owing to the encapsulation of Cdots into MOFs frameworks, the polar functional groups on the Cdots surface have a prominent and positive impact on H_2 storage capacity compared to pristine MOFs.

Experimental section

Materials

N,*N*-Diethylformamide (DEF), terephtalic acid (bdc), 1,3,5-tris(4-carboxyphenyl)benzene (btb), citric acid, urea, $Zn(NO_3)_2{\cdot}6H_2O$ and other chemicals were purchased from Sigma-Aldrich and used without further purification.

Characterization

Transmission electron microscopy (TEM) and high-resolution (HRTEM) images were taken on a JEOL-2100F apparatus at an accelerating voltage of 200 kV. The surface morphologies of the carbon materials were examined by a scanning electron microscope (SEM, JSM-7600F) at an acceleration voltage of 10 kV. The energy dispersive spectroscopy (EDS) was taken on JSM-5160LV-Vantage type energy spectrometer. The powder X-Ray diffraction (XRD) patterns were recorded on a D/max 2500VL/PC diffractometer (Japan) equipped with graphite monochromatized Cu Kα radiation (λ = 1.54060 Å). The corresponding work voltage and current was 40 kV and 100 mA, respectively. The nitrogen adsorption–desorption experiments were operated at 77 K on a Micromeritics ASAP 2050 system. Prior to the measurement, the samples were degassed at 90 °C for 10 hours. Ultraviolet-visible (UV-vis) absorption spectra were obtained on Cary 60 spectrophotometer (Agilent). Photoluminescence (PL) spectra were recorded on LS 50B (Perkin-Elmer). Atomic force microscopy (AFM) images were recorded with a Nanoscope IIIa scanning probe microscope (Agilent, USA) using a tapping mode. Fourier transform infrared (FTIR) spectra were acquired in the range of 400–4000 cm^{-1} on a Tensor 27 (Bruker, Germany) at room temperature. Confocal laser scanning microscopy (CLSM) was operated on an Olympus Fluo-view FV1000.

Preparation of Cdots

Cdots were synthesized according to the reported literature.[17] Citric acid (3 g) and urea (3 g) were added to 10 mL distilled water to form a transparent solution. Then, the solution was heated in a 750 W microwave oven for 5 min until the colorless solution finally changed into a dark-brown clustered solid, exhibiting the formation of Cdots. The obtained product was heated at 60 °C for 1 h in a vacuum oven in order to remove the residual small molecules. The Cdots solution was purified through centrifugation at 3000 rpm for 20 min in favor of removing large or agglomerated particles.

Preparation of Cdots@MOFs

Cdots@MOFs were synthesized by a stepwise synthetic method. First, 5 mL of DEF solution consisting of bdc (0.016 g) or btb (0.02 g) or bdc (0.02 g) and btb (0.0438 g) and $Zn(NO_3)_2{\cdot}6H_2O$ (0.09 g) were thoroughly dissolved by ultrasonication. Subsequently, the solution was heated to 90 °C and maintained at this temperature until the MOF crystals were formed. The MOF mother solution was filtered and cooled down to room temperature. Then, 0.5 mL of Cdots solution was added into the filtered solution and incubated at room temperature for 12 h. The obtained MOF crystals were preserved in a DEF solution, which were denoted as Cdots@MOF-5, Cdots@MOF-177, and Cdots@UMCM-1a, respectively.

In the control experiments, MOF-5, MOF-177, and UMCM-1 were prepared by a solvothermal approach according to the reported method.[18] 5 mL of DEF solution consisting of bdc (0.016 g) or btb (0.02 g) or bdc (0.02 g) and btb (0.0438 g) and $Zn(NO_3)_2{\cdot}6H_2O$ (0.09 g) were thoroughly dissolved by ultrasonication. Then, the mixture was placed in a Teflon reactor and heated at 85 °C for 3 days, and then it was gradually cooled to room temperature. For comparison, Cdots@UMCM-1b were prepared as follows: 0.5 mL of Cdots was added into 5 mL of DEF consisting of bdc (0.016 g) and btb (0.0438 g) and $Zn(NO_3)_2{\cdot}6H_2O$ (0.09 g), as per the abovementioned procedure under identical conditions.

Results and discussion

As can be seen from Fig. 1A, the TEM image of the Cdots clearly indicates that most of the Cdots are spherical with sizes <6 nm. The HRTEM image (inset of Fig. 1A) reveals the high crystallinity of the Cdots. The elemental compositions of the Cdots were investigated by EDS. Fig. 1B shows that the Cdots mainly consist of carbon, nitrogen and oxygen. From Fig. 1C–D, the AFM image also suggests that the topographic height of the Cdots is in the range of 1–6 nm with an average diameter of about 3.5 nm, which is consistent with that achieved by TEM. The FTIR spectrum of the Cdots is presented in Fig. 1E, which demonstrates the existence of C═O, COO–, O–H, N–H, C–H and C–N. To evaluate the optical properties of the Cdots, the corresponding UV-vis absorption and PL emission spectra of a DEF solution of Cdots were monitored. As shown in Fig. 1F, the UV-vis spectrum gives a

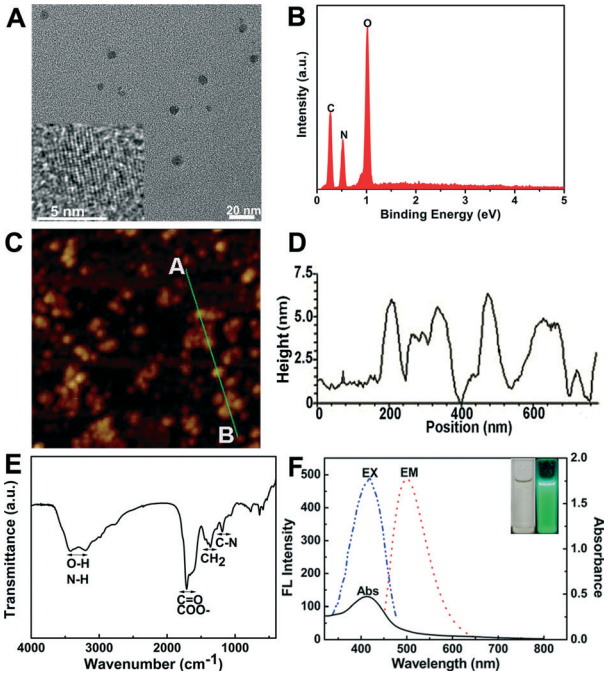

Fig. 1 (A) TEM image of the prepared Cdots, and the inset shows the HRTEM image of individual Cdot. (B) EDS of the Cdots. (C) AFM image of the Cdots on a mica substrate. (D) The height profile along line AB in the image. (E) FTIR spectrum of the Cdots in the dry state. (F) UV-vis absorption (black line), PL excitation (blue line) and emission (red line) spectra of Cdots solution. The photograph was taken without (left) and with (right) UV light (365 nm).

broad peak centered at 420 nm. Upon excitation at the absorption band of 420 nm, the strong PL emission of the Cdots appears at 500 nm, which is in agreement with the previous literature.[17] Notably, the green fluorescence of the Cdots is strong enough to be easily seen with the naked eyes under a UV light with a wavelength 365 nm (the inset of Fig. 1F).

The optical micrographs of UMCM-1 and Cdots@UMCM-1a are presented in Fig. 2A–B, respectively. The classical needle-like crystals are visible and reveal the high crystallinity of the products. The SEM image of Cdots@UMCM-1a (the inset of Fig. 2B) also supports the above results. In particular, it is clearly seen that the crystal sizes of Cdots@UMCM-1a are smaller than that of UMCM-1. As can be seen from Fig. S1 (ESI†), the PXRD patterns of the synthesized crystals are almost identical with those simulated, proving that the framework structures remain almost intact and the assembly process of UMCM-1 crystals is not disturbed by the encapsulation of the Cdots. In comparison to the strong peaks of the UMCM-1 crystals, the peaks of the Cdots are not obviously found, presumably by virtue of their low concentrations and/or small sizes hosted by the UMCM-1 matrix.[9e,13a,c,19] Fig. 2C–D shows the TEM and HRTEM images of Cdots@UMCM-1a after sonication, respectively. The HRTEM image indicates that the lattice spacing is 0.209 nm, which agrees well with the (100) diffraction plane of graphite. Moreover, compared to the original UMCM-1 (Fig. S2A, ESI†), the EDS (Fig. S2B, ESI†) reveals that Cdots@UMCM-1a are composed of the

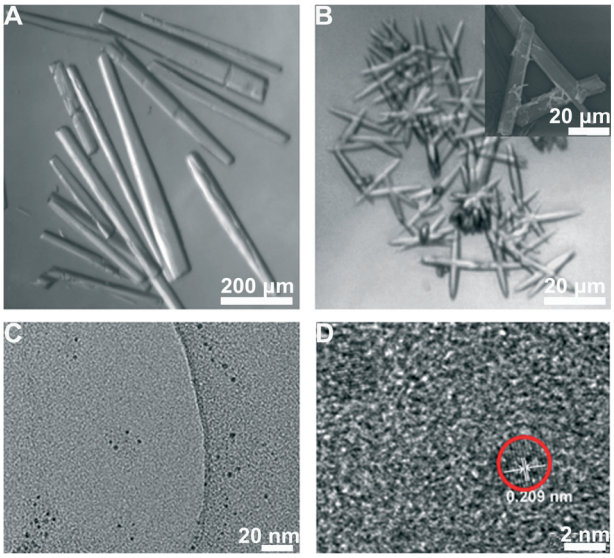

Fig. 2 Optical micrographs of (A) UMCM-1 and (B) Cdots@UMCM-1a (inset: SEM of Cdots@UMCM-1a). (C) TEM and (D) HRTEM of Cdots@UMCM-1a after sonication.

C, N, Zn, and O elements. These results further confirm that the Cdots are successfully embedded within UMCM-1.

The optical properties of the Cdots@UMCM-1a composites were explored by PL spectroscopy at room temperature. Fig. 3A indicates that the DEF solution of UMCM-1 appears to have no luminescence when excited at 420 nm. On the contrary, with an identical excitation wavelength, the DEF solution of Cdots@UMCM-1a shows high fluorescence located at approximately 500 nm (Fig. 3B). It efficiently proves that the green luminescence only originates from Cdots. In comparison with UMCM-1 (inset of Fig. 3A), the fluorescence of the DEF solution of Cdots@UMCM-1a at the illumination of UV light (365 nm) can be obviously seen in the inset of Fig. 3B. However, the difference of color in Fig. 1F and 3B is

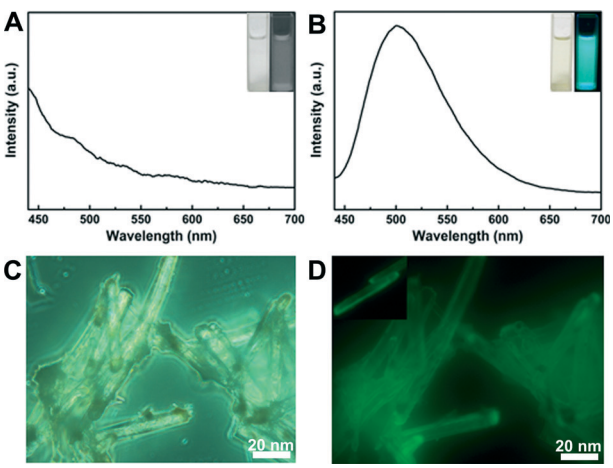

Fig. 3 PL spectra of (A) UMCM-1 and (B) Cdots@UMCM-1a with excitation wavelength at 420 nm (insets: photographs of corresponding samples without (left) and with (right) UV light (365 nm)). (C) and (D) CLSM images of Cdots@UMCM-1a.

attributed to the different content of Cdots in Cdots@UMCM-1a and the original Cdots solution. Note that the content of Cdots in Cdots@UMCM-1a is much lower than that of the original Cdots solution. Moreover, the characteristic emission peak of Cdots@UMCM-1a excited at 420 nm is in accordance with that of Cdots. Therefore, this confirms that the Cdots in Cdots@UMCM-1a have an analogous state to that in the mother solution. Furthermore, UMCM-1 shells are formed fast enough to effectively prevent Cdots aggregation after the addition of the Cdots into the supersaturated UMCM-1 mother solution.[15] As mentioned above, these data sufficiently demonstrate that the Cdots are successfully incorporated into the frameworks of UMCM-1 and still retain the highly luminescent properties of Cdots.

To further access the stability of the Cdots inside Cdots@UMCM-1a, the fluorescent performance of Cdots@UMCM-1a under laboratory conditions for more than one month was investigated by CLSM. From Fig. 3C–D, the strong fluorescence could be observed by naked eyes. Hence, this result specifies that the Cdots are so stable inside the Cdots@UMCM-1a composites and that the luminescent intensity, compared to the original Cdots, does not change. Based on these considerations, we propose the growth mechanisms as follows: 1) the carboxylate groups at the surface of the Cdots are effectively combined with Zn^{2+} from the mother solution, and 2) as crystallization seeds, Cdots can induce the nucleation and control growth of UMCM-1. Moreover, Cdots are spontaneously embedded into the Cdots@UMCM-1 matrix.[10d,13a,15,20]

When Cdots are encapsulated into the MOFs matrix, how can they affect gas storage, increase or decrease? To address this issue, gas adsorption was employed to investigate the changes of storage capacity of Cdots@UMCM-1a. For comparison, the gas sorption isotherms for UMCM-1 and Cdots@UMCM-1b are also presented in Fig. 4. The N_2 sorption isotherms of these samples are classified as a type IV (Fig. 4A), characteristic of a micro/meso-porous structure, as also supported by the pore size distributions analyzed by the DFT methods (Fig. S3, ESI†).[21] However, compared with the original UMCM-1, it is surprising that the surface areas of Cdots@UMCM-1 (a and b) decrease and the H_2 storage capacities of Cdots@UMCM-1 (a and b) are oppositely enhanced when Cdots are embedded into the frameworks of UMCM-1. Note that the enhancement in H_2 sorption capacities is about 9%. The detailed data are summarized in Table S1 (ESI†). Generally, the interactions between the frameworks and H_2 molecules decrease along with increase in the pore volumes. Hence, the large pore volumes of MOFs are not crucial factors for increasing the H_2 storage at ambient pressure.[22] Considering the above experimental results, we think that the specific interactions between polar functional groups (such as –COOH and –OH) at the Cdots surface and H_2 molecules are beneficial to enhance H_2 storage.[10d,23] Particularly, according to the H_2 sorption data of UMCM-1 and Cdots@UMCM-1a at 77 K and 87 K (Fig. S4, ESI†), the isosteric heat of H_2 adsorption of Cdots@UMCM-1a is about

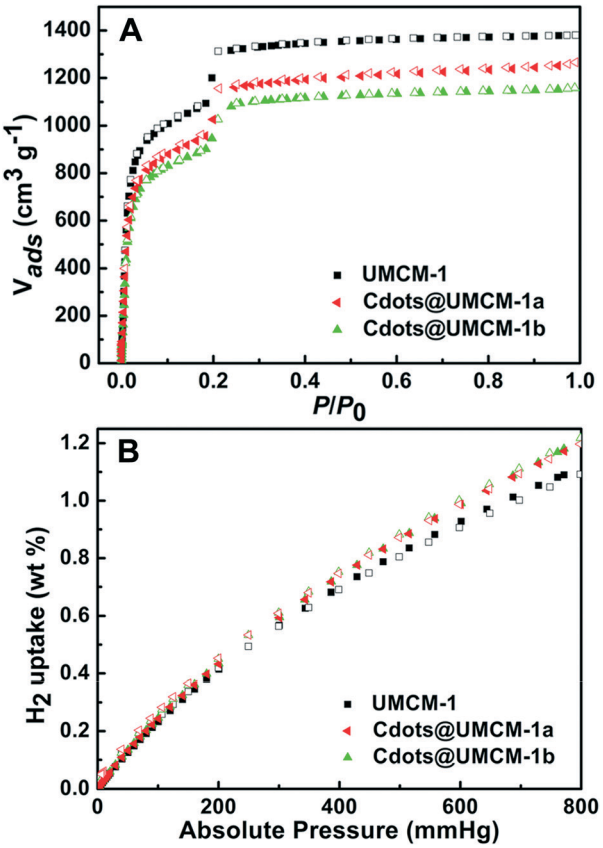

Fig. 4 (A) N_2 and (B) H_2 sorption isotherms for UMCM-1, Cdots@UMCM-1a, and Cdots@UMCM-1b.

5.6 kJ mol^{-1}, which is higher than that of UMCM-1 (5.2 kJ mol^{-1}). This further supports the above conclusion. To our knowledge, this is the first example of Cdots functional MOFs, which efficiently increase H_2 sorption capacity.

In addition, the fluorescence properties of Cdots@UMCM-1a inspired us to exploit the potential applications in detection of organic molecules. In brief, a certain amount of these composites was immersed in the corresponding solution, forming stable suspensions by sonication. The solvents were DEF, *N*,*N*-dimethylformamide (DMF), *N*,*N*-dimethylacetamide (DMA), methanol, ethanol, and nitrobenzene (NB). As shown in Fig. 5A, the predominant emission peak and intensity are obviously different when Cdots@UMCM-1a composites are dispersed in different solvents. For example, the emission peak of Cdots@UMCM-1a in a DEF solution is presented at 500 nm when excited at 420 nm. On the other hand, the emission peaks in DMF, methanol, ethanol, DMA, and NB solutions are presented at about 496, 508, 488, 487, and 486 nm, respectively. Moreover, the intensities of Cdots@UMCM-1a in these solvents decrease compared to that in the DEF solution. The vastly different luminescent responses of solvents may be related to solvent polarity and the physical interaction of solvent and solute. The intact frameworks of Cdots@UMCM-1a in different solvents were confirmed by the comparative PXRD (Fig. S5, ESI†). To further evaluate sensing sensitivity toward nitroaromatic explosives in detail,

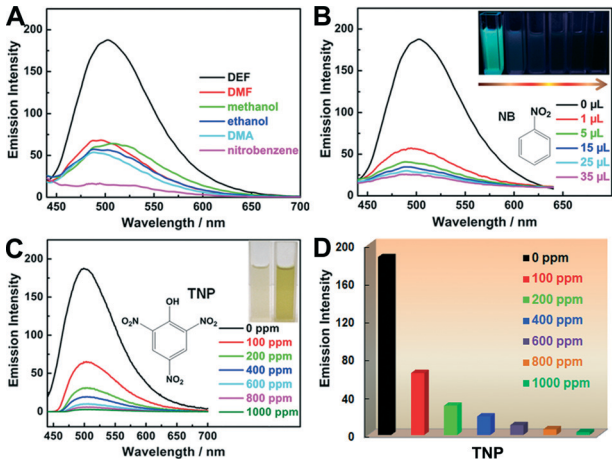

Fig. 5 (A) Emission spectra of Cdots@UMCM-1a in different solvents (excited at 420 nm). (B) Emission spectra of Cdots@UMCM-1a in DEF solution with different amounts of NB (excited at 420 nm). Inset in (B): a photograph taken under UV light (365 nm). (C) Emission spectra and (D) corresponding emission intensities of Cdots@UMCM-1a in DEF solution with different concentration of TNP (excited at 420 nm). Inset in (C): color changes before and after incremental addition of TNP (left: Cdots@UMCM-1a in DEF; right: Cdots@UMCM-1a in DEF containing TNP).

the emissive responses were monitored with a different amount of NB or 2,4,6-trinitrophenol (TNP) added to the DEF suspensions of Cdots@UMCM-1a (Fig. 4B–C). Fig. S6 (ESI†) indicates the PL quenching up to approximately one sixth of the initial intensity in the DEF solution with 35 μL of NB. Moreover, the fluorescence change can be observed under a UV lamp (365 nm) in the inset of Fig. 4B. In terms of TNP, when the concentration of TNP was 1000 ppm in DEF suspension of Cdots@UMCM-1a, the luminescence was completely quenched. Interestingly, the color of the corresponding solution turned orange, which could be seen by the naked eyes (Fig. 4C). Therefore, TNP can be conveniently and rapidly detected by recording the color change. The relationship between emissive responses and amounts of NB or TNP in DEF solution of Cdots@UMCM-1a is shown in Fig. S7 (ESI†). Taking into account the above results, the possible mechanism of fluorescence quenching is speculated to be that electron transfer from the electron-donating of amino groups at the surface of the Cdots to the electron-deficient NB or TNP molecules can occur, resulting in fluorescence quenching. In a control experiment, the DEF solution of Cdots having the similar intensity with that of Cdots@UMCM-1a composites was also added 35 μL of NB or 1000 ppm of TNP. As can be seen from Fig. S8 (ESI†), the fluorescence response of Cdots@UMCM-1a is much more sensitive than that of Cdots, further suggesting that Cdots@MOFs have highly sensitive ability than Cdots solely dispersed in a DEF solution. This work represents the first report of Cdots@UMCM-1a as an enhanced fluorescent sensor for nitroaromatic explosives. The PXRD pattern further suggests that the framework is unbroken after the detection of NB or TNP (Fig. S9, ESI†).

To examine the universality of our proposed encapsulation strategy, Cdots were also incorporated into MOF-5 and MOF-177 by following the similar method of Cdots@UMCM-1a,[18] respectively. These obtained composites were further characterized by SEM, PXRD, EDS, PL and CLSM, respectively (Fig. S10–15, ESI†). All the data are similar to those of Cdots@UMCM-1a. The aforementioned results efficiently prove that the stepwise synthetic approach is efficient and universal for preparing smaller-sized Cdots@MOFs.

Conclusions

In summary, for the first time, we have successfully fabricated novel smaller-sized Cdots@MOFs composites by a stepwise synthetic approach. The fluorescent performance of the hybrid under laboratory conditions for more than one month was still retained. As expected, the polar functional groups at the surface of Cdots have significant effects on the H_2 storage capacity of corresponding hybrids. Furthermore, as a fluorescent sensor, Cdots@UMCM-1a showed the sensitive fluorescent sensing for nitroaromatic explosives because of the double effect of MOFs and Cdots. The combination of nanoparticles and MOFs will provide a new direction to synthesize novel and multifunctional hybrid composites and take advantage of the synergetic effect of both nanoparticles and MOFs, and further work is currently underway in this regard.

Acknowledgements

This work was financially supported by the NSFC (no. 21175069, 21371099, 21471080, and 21475062), the program of Jiangsu Specially Appointed Professor, the NSF of Jiangsu Province of China (no. BK20130043), the Natural Science Research of Jiangsu Higher Education Institutions of China (no. 13KJB150021), the Priority Academic Program Development of Jiangsu Higher Education Institutions, the Foundation of Jiangsu Collaborative Innovation Center of Biomedical Functional Materials and the Youths Science Foundation of Jining University (no. 2014QNKJ08).

Notes and references

1 (*a*) H. L. Jiang and Q. Xu, *Chem. Commun.*, 2011, **47**, 3351; (*b*) H. C. Zhou, J. R. Long and O. M. Yaghi, *Chem. Rev.*, 2012, **112**, 673; (*c*) Y. Cui, Y. Yue, G. Qian and B. Chen, *Chem. Rev.*, 2011, **112**, 1126.

2 (*a*) H. Furukawa, N. Ko, Y. B. Go, N. Aratani, S. B. Choi, E. Choi, A. O. Yazaydin, R. Q. Snurr, M. O'Keeffe, J. Kim and O. M. Yaghi, *Science*, 2010, **329**, 424; (*b*) W. Xuan, C. Zhu, Y. Liu and Y. Cui, *Chem. Soc. Rev.*, 2012, **41**, 1677.

3 O. M. Yaghi, M. O'Keeffe, N. W. Ockwig, H. K. Chae, M. Eddaoudi and J. Kim, *Nature*, 2003, **423**, 705.

4 S. Kitagawa, R. Kitaura and S. Noro, *Angew. Chem., Int. Ed.*, 2004, **43**, 2334.

5 J.-R. Li, R. J. Kuppler and H.-C. Zhou, *Chem. Soc. Rev.*, 2009, **38**, 1477.

6 C. Wang, D. Liu and W. Lin, *J. Am. Chem. Soc.*, 2013, **135**, 13222.
7 P. Horcajada, T. Chalati, C. Serre, B. Gillet, C. Sebrie, T. Baati, J. F. Eubank, D. Heurtaux, P. Clayette, C. Kreuz, J.-S. Chang, Y. K. Hwang, V. Marsaud, P.-N. Bories, L. Cynober, S. Gil, G. Ferey, P. Couvreur and R. Gref, *Nat. Mater.*, 2010, **9**, 172.
8 (*a*) A. Dhakshinamoorthy and H. Garcia, *Chem. Soc. Rev.*, 2012, **41**, 5262; (*b*) J. Juan-Alcaniz, J. Gascon and F. Kapteijn, *J. Mater. Chem.*, 2012, **22**, 10102; (*c*) R. Ricco, L. Malfatti, M. Takahashi, A. J. Hill and P. Falcaro, *J. Mater. Chem. A*, 2013, **1**, 13033; (*d*) C. M. Doherty, D. Buso, A. J. Hill, S. Furukawa, S. Kitagawa and P. Falcaro, *Acc. Chem. Res.*, 2013, **47**, 396; (*e*) M. L. Foo, R. Matsuda and S. Kitagawa, *Chem. Mater.*, 2013, **26**, 310; (*f*) H. R. Moon, D. W. Lim and M. P. Suh, *Chem. Soc. Rev.*, 2013, **42**, 1807.
9 (*a*) A. Aijaz, A. Karkamkar, Y. J. Choi, N. Tsumori, E. Ronnebro, T. Autrey, H. Shioyama and Q. Xu, *J. Am. Chem. Soc.*, 2012, **134**, 13926; (*b*) F. Schröder, D. Esken, M. Cokoja, M. W. E. van den Berg, O. I. Lebedev, G. Van Tendeloo, B. Walaszek, G. Buntkowsky, H.-H. Limbach, B. Chaudret and R. A. Fischer, *J. Am. Chem. Soc.*, 2008, **130**, 6119; (*c*) T.-H. Park, A. J. Hickman, K. Koh, S. Martin, A. G. Wong-Foy, M. S. Sanford and A. J. Matzger, *J. Am. Chem. Soc.*, 2011, **133**, 20138; (*d*) L. He, Y. Liu, J. Liu, Y. Xiong, J. Zheng, Y. Liu and Z. Tang, *Angew. Chem., Int. Ed.*, 2013, **52**, 3741; (*e*) G. Lu, S. Z. Li, Z. Guo, O. K. Farha, B. G. Hauser, X. Y. Qi, Y. Wang, X. Wang, S. Y. Han, X. G. Liu, J. S. DuChene, H. Zhang, Q. C. Zhang, X. D. Chen, J. Ma, S. C. J. Loo, W. D. Wei, Y. H. Yang, J. T. Hupp and F. W. Huo, *Nat. Chem.*, 2012, **4**, 310; (*f*) Y. Yang, F. Wang, Q. Yang, Y. Hu, H. Yan, Y.-Z. Chen, H. Liu, G. Zhang, J. Lu, H.-L. Jiang and H. Xu, *ACS Appl. Mater. Interfaces*, 2014, **6**, 18163; (*g*) Y.-Z. Chen, Q. Xu, S.-H. Yu and H.-L. Jiang, *Small*, 2014, DOI: 10.1002/smll.201401875.
10 (*a*) C. Petit and T. J. Bandosz, *J. Mater. Chem.*, 2009, **19**, 6521; (*b*) C. Petit and T. J. Bandosz, *Adv. Mater.*, 2009, **21**, 4753; (*c*) M. Jahan, Z. Liu and K. P. Loh, *Adv. Funct. Mater.*, 2013, **23**, 5363; (*d*) R. Kumar, K. Jayaramulu, T. K. Maji and C. N. Rao, *Chem. Commun.*, 2013, **49**, 4947.
11 (*a*) S. J. Yang, J. Y. Choi, H. K. Chae, J. H. Cho, K. S. Nahm and C. R. Park, *Chem. Mater.*, 2009, **21**, 1893; (*b*) Z. Xiang, X. Peng, X. Cheng, X. Li and D. Cao, *J. Phys. Chem. C*, 2011, **115**, 19864.
12 (*a*) J. Song, Z. Luo, D. K. Britt, H. Furukawa, O. M. Yaghi, K. I. Hardcastle and C. L. Hill, *J. Am. Chem. Soc.*, 2011, **133**, 16839; (*b*) Q. Han, C. He, M. Zhao, B. Qi, J. Niu and C. Duan, *J. Am. Chem. Soc.*, 2013, **135**, 10186.
13 (*a*) D. Buso, J. Jasieniak, M. D. Lay, P. Schiavuta, P. Scopece, J. Laird, H. Amenitsch, A. J. Hill and P. Falcaro, *Small*, 2012, **8**, 80; (*b*) S. Jin, H. J. Son, O. K. Farha, G. P. Wiederrecht and J. T. Hupp, *J. Am. Chem. Soc.*, 2013, **135**, 955; (*c*) D. Esken, S. Turner, C. Wiktor, S. B. Kalidindi, G. Van Tendeloo and R. A. Fischer, *J. Am. Chem. Soc.*, 2011, **133**, 16370; (*d*) B. P. Biswal, D. B. Shinde, V. K. Pillai and R. Banerjee, *Nanoscale*, 2013, **5**, 10556.
14 (*a*) L. Zheng, Y. Chi, Y. Dong, J. Lin and B. Wang, *J. Am. Chem. Soc.*, 2009, **131**, 4564; (*b*) C. Ding, A. Zhu and Y. Tian, *Acc. Chem. Res.*, 2013, **47**, 20.
15 K. Sugikawa, S. Nagata, Y. Furukawa, K. Kokado and K. Sada, *Chem. Mater.*, 2013, **25**, 2565.
16 K. Khaletskaya, J. Reboul, M. Meilikhov, M. Nakahama, S. Diring, M. Tsujimoto, S. Isoda, F. Kim, K. I. Kamei, R. A. Fischer, S. Kitagawa and S. Furukawa, *J. Am. Chem. Soc.*, 2013, **135**, 10998.
17 S. Qu, X. Wang, Q. Lu, X. Liu and L. Wang, *Angew. Chem., Int. Ed.*, 2012, **51**, 12215.
18 K. Koh, A. G. Wong-Foy and A. J. Matzger, *Angew. Chem., Int. Ed.*, 2008, **47**, 677.
19 P. Wang, J. Zhao, X. Li, Y. Yang, Q. Yang and C. Li, *Chem. Commun.*, 2013, **49**, 3330.
20 T. Tsuruoka, H. Kawasaki, H. Nawafune and K. Akamatsu, *ACS Appl. Mater. Interfaces*, 2011, **3**, 3788.
21 S. J. Yang, J. H. Im, H. Nishihara, H. Jung, K. Lee, T. Kyotani and C. R. Park, *J. Phys. Chem. C*, 2012, **116**, 10529.
22 M. P. Suh, H. J. Park, T. K. Prasad and D.-W. Lim, *Chem. Rev.*, 2011, **112**, 782.
23 S. Liu, L. Sun, F. Xu, J. Zhang, C. Jiao, F. Li, Z. Li, S. Wang, Z. Wang, X. Jiang, H. Zhou, L. Yang and C. Schick, *Energy Environ. Sci.*, 2013, **6**, 818.